Structural and Functional Characterization of Bc28.1, Major Erythrocyte-binding Protein from Babesia canis Merozoite Surface

Yin-Shan Yang, Brice Murciano, Karina Moubri, Prisca Cibrelus, Theo Schetters, André Gorenflot, Stéphane Delbecq, Christian Roumestand

THE JOURNAL OF BIOLOGICAL CHEMISTRY VOL. 287, NO. 12, pp. 9495–9508, March 16, 2012

Structural and Functional Characterization of Bc28.1, Major Erythrocyte-binding Protein from *Babesia canis* Merozoite Surface*[S]

Received for publication, May 16, 2011, and in revised form, January 16, 2012 Published, JBC Papers in Press, January 31, 2012, DOI 10.1074/jbc.M111.260745

Yin-Shan Yang[‡§1], Brice Murciano[‡§¶2], Karina Moubri[¶], Prisca Cibrelus[¶], Theo Schetters[‖], André Gorenflot[¶], Stéphane Delbecq[¶1], and Christian Roumestand[‡§3]

From the [‡]Centre de Biochimie Structurale, CNRS UMR 5048, Université Montpellier 1 et 2, F34090 Montpellier, France, [§]INSERM U1054, F34090 Montpellier, France, [¶]EA4558, Vaccination Antiparasitaire, Université de Montpellier 1, Faculté de Pharmacie, F34093 Montpellier Cedex 5, France, and the [‖]Department of Parasitology, Intervet International B.V., Boxmeer 5830AA, The Netherlands

Babesiosis (formerly known as piroplasmosis) is a tick-borne disease caused by the intraerythrocytic development of protozoa parasites from the genus *Babesia*. Like *Plasmodium falciparum*, the agent of malaria, or *Toxoplasma gondii*, responsible for human toxoplasmosis, *Babesia* belongs to the Apicomplexa family. *Babesia canis* is the agent of the canine babesiosis in Europe. Clinical manifestations of this disease range from mild to severe and possibly lead to death by multiple organ failure. The identification and characterization of parasite surface proteins represent major goals, both for the understanding of the Apicomplexa invasion process and for the vaccine potential of such antigens. Indeed, we have already shown that Bd37, the major antigenic adhesion protein from *Babesia divergens*, the agent of bovine babesiosis, was able to induce complete protection against various parasite strains. The major merozoite surface antigens of *Babesia canis* have been described as a 28-kDa membrane protein family, anchored at the surface of the merozoite. Here, we demonstrate that Bc28.1, a major member of this multigenic family, is expressed at high levels at the surface of the merozoite. This protein is also found in the parasite *in vitro* culture supernatants, which are the basis of effective vaccines against canine babesiosis. We defined the erythrocyte binding function of Bc28.1 and determined its high resolution solution structure using NMR spectroscopy. Surprisingly, although these proteins are thought to play a similar role in the adhesion process, the structure of Bc28.1 from *B. canis* appears unrelated to the previously published structure of Bd37 from *B. divergens*. Site-directed mutagenesis experiments also suggest that the mechanism of the interaction with the erythrocyte membrane could be different for the two proteins. The resolution of the structure of Bc28 represents a milestone for the characterization of the parasite erythrocyte binding and its interaction with the host immune system.

The phylum Apicomplexa, a large group of single-celled eukaryotic intracellular parasites, includes some of the most important pathogenic parasites of humans and animals, the deadliest of which is the malaria parasite *Plasmodium falciparum*, responsible for one million human deaths per year and with almost half of the human population at risk of contracting malaria. No vaccine currently exists against *P. falciparum*, and parasites are becoming increasingly resistant to pharmaceuticals. This is also true for other pathogenic Apicomplexa, such as *Toxoplasma*, which, together with *Plasmodium*, challenge global human health improvement programs, and coccidiosis and babesiosis are detrimental for agri-business in both industrialized and developing countries. Babesiosis (formerly known as piroplasmosis) is a tick-borne disease caused by the intraerythrocytic development of an Apicomplexa from the *Babesia* genus. Hemolytic anemia due to parasite development leads to major symptoms, such as hemoglobinury, fever, asthenia, and renal failure. Among other animals, domestic dogs are susceptible to several species, mainly from the so-called large *Babesia* (in contrast to smaller *Babesia*, such as *Babesia gibsoni*): *Babesia canis* in Europe, *Babesia rossi* in Africa, and *Babesia vogeli* in tropical and subtropical regions around the world. Clinical manifestations range from mild to severe and can lead to death by multiple organ failure (1).

The search for an efficient recombinant vaccine against Apicomplexa parasites requires the identification of high potential antigen candidates. Such antigens are molecules originating from parasites, which could be targeted by the immune system to at least limit the parasitic infection and its consequences. One of the methods for finding antigen candidates relies on the identification of molecules recognized by the immune system of individuals that recovered from parasitic infection. In another approach, target molecules can be chosen from those that are involved in critical life processes of the parasite; invasion of the host cell by the parasite represents one such process. Because Apicomplexa are intracellular parasites, the most accessible antigens are found at the surface of transitory extra-

* This work was supported in part by a grant from Intervet International B.V. This work (very high-field NMR at 950 MHz) was also supported by Très Grands Equipments de Résonance Magnétique Nucléaire à Très Haut Champs Fr3050.

The atomic coordinates and structure factors (code 2lcu) have been deposited in the Protein Data Bank, Research Collaboratory for Structural Bioinformatics, Rutgers University, New Brunswick, NJ (http://www.rcsb.org/).

[S] This article contains supplemental Figs. 1–3.

[1] Both authors contributed equally to this work.

[2] Ph.D. student supported by an "Axes Prioritaires" grant from Ministere de l'Enseignement Superieur et de la Recherche.

[3] To whom correspondence should be addressed: Centre de Biochimie Structurale, 29 Route de Navacelles, 34090 Montpellier, France. Tel.: 33-467-417-704; Fax: 33-467-417-913; E-mail: christian.roumestand@cbs.cnrs.fr.

cellular forms like merozoites, after host cell egress and before or during the invasion of the next host cell. Targeting the merozoite surface by recombinant vaccines has been proved to be relatively efficient against malaria (2).

Adhesive proteins at the surface of Apicomplexa infective stages are involved in the first step of host cell invasion. Some of these interacting proteins contain domains conserved through a large panel of organisms, ranging from bacteria to mammals, as well as parasite-specific architecture. In several parasites, lineage-specific expansion of some of these interacting domains had led to large protein repertoires, as exemplified by the SAG1 (surface antigen 1) family in *Toxoplasma gondii* or the DBL (Duffy binding-like) domain in *P. falciparum* (3). As in many other parasites, the surface of Apicomplexa infective stages is coated mainly by GPI[4]-anchored proteins (4, 5). In contrast to transmembrane proteins, such as TRAP or AMA1, essentially conserved in all Apicomplexa (6), the diversity of GPI-anchored protein repertoires appears to depend on the Apicomplexa genus. Although the surface of *Toxoplasma* tachyzoites is mainly coated by proteins from the SRS family (7) and SUSA family (8), 16 different GPI-anchored proteins are found at the merozoite surface in *P. falciparum* (9).

In contrast to the high diversity of GPI-anchored proteins found in *Toxoplasma* and *Plasmodium*, ranging from 20 to more than 150 kDa, and generated by a high copy number multigenic family, the GPI-anchored protein repertoire of *Babesia* appears to be less complex. In the recently sequenced genome of *Babesia bovis*, only the five genes of the already known variable merozoite surface antigen were found (6). In *B. canis* and *Babesia divergens*, in the absence of genomic data, only the small erythrocyte-binding protein Bc28 and Bd37 families are currently known (10).

In previous studies, we have shown that immunization with recombinant Bd37, the major antigenic adhesion GPI-anchored protein from *B. divergens*, was able to induce complete protection against various parasite polymorphic strains (11). The intraerythrocytic protozoa *B. divergens* is the agent of bovine babesiosis in Europe. We previously solved the solution structure of this erythrocyte-binding protein. It suggests that conformational plasticity could be functionally and/or immunologically important (12). In an attempt to find Bd37 homologues in *B. canis*, amplifications by low specificity PCR using Bd37-derived primers were performed on parasite DNA, leading to the identification of the Bc28 protein family. These proteins are in the 28 kDa range and do not show any clear sequence homology with the Bd37 protein family (in which currently two members were identified), suggesting structural divergence (10).

In this report, we present the atomic structure as well as the erythrocyte binding function of Bc28.1 from *B. canis*, the major member of the Bc28 multigenic family. In agreement with the low sequence homology, our data reveal an apparently unrelated structure when compared with Bd37 from *B. divergens*, although the two proteins are thought to play a similar role in the two organisms. In addition, site-directed mutagenesis experiments suggest that Bc28.1 and Bd37 might bind to the erythrocyte membrane through different mechanisms, at least in the early stages of the association.

EXPERIMENTAL PROCEDURES

Parasite in Vitro Culture and Monoclonal Antibody Production—In vitro culture of *B. canis* strain A parasites was previously described, using erythrocytes from dogs housed in a dedicated facility (agreement B 34-175-17). Briefly, continuous cultures of parasites were performed in RPMI 1640 medium (Invitrogen) containing 10% dog serum and 2% (packed cell volume) dog erythrocytes. Erythrocyte ghosts were obtained by freeze-thawing cycles followed by several washes of membranes with phosphate-buffered saline until hemoglobin has been removed. Ghosts were then boiled in SDS-PAGE reducing sample buffer.

From a previous screen of monoclonal antibodies raised against purified merozoites from *B. canis*,[5] the mAb 6C9 was selected as recognizing a 28-kDa merozoite surface antigen. The hybridoma secreting the 6C9 antibody was recloned by limiting dilution and expanded in Opti-MEM medium (Invitrogen) containing 5% fetal bovine serum. Cells were then transferred in a CELLine two-compartment bioreactor (Integra Biosciences) for large scale production in aseric conditions, and cell culture supernatant was harvested weekly, sterile-filtered, and frozen at −20 °C until use.

Growth Inhibition Assay—B. canis parasites were cultivated in 24-well plates in 800 μl of RPMI 1640 containing 10% dog serum. Rabbit serum directed against Bc28.1 was added (10% volume) and the corresponding preimmune serum was used as a negative control. An unrelated serum (anti-BcVir15, 8%) previously shown to induce parasite growth inhibition was used as a positive control. The monoclonal 6C9 was purified using ion exchange chromatography and dialyzed against PBS. Purified mAb was added at 1 mg/ml to the culture, and an unrelated mAb produced in similar conditions was used as a control. Each culture was done in triplicate, and medium replacement with appropriate antibodies was done after 24 h of incubation. The parasitemia in each culture was assessed by thin blood smears after an additional 24 h of incubation.

Merozoite Purification and Protein Fractionation Based on Membrane Properties—Infective *B. canis* merozoites have been purified using streptolysin O-mediated lysis of parasitized red blood cells followed by differential centrifugation. Starting from *in vitro* culture, dog erythrocytes were washed three times with RPMI 1640. The streptolysin O (La Technique Biologique) was added to the packed red blood cells at 0.025 units/μl, and then 8 volumes of RPMI 1640 was added to 1 volume of packed red blood cells. After 10 min at 37 °C, the cell suspension was centrifuged (10 min, 300 × *g*), and supernatant was centrifuged for 30 min at 1100 × *g*. The pellet contains purified, infective merozoites, whereas supernatant was called soluble fraction, which mainly represents the erythrocyte cytoplasm.

Phase partitioning using Triton X-114 was performed essentially according to Bordier (13). Briefly, cell pellets were solubi-

[4] The abbreviations used are: GPI, glycosylphosphatidylinositol; TRITC, tetramethylrhodamine isothiocyanate.

[5] Y.-S. Yang, B. Murciano, K. Moubri, P. Cibrelus, T. Schetters, A. Gorenflot, S. Delbecq, and C. Roumestand, unpublished data.

lized in 10 volumes of 2% precondensed Triton X-114 (Fluka) in Tris-buffered saline, and soluble fractions were brought to 2% Triton X-114 by the addition of 11.4% solution in TBS. After incubation on ice for 1 h, solutions were centrifuged at 13,000 × *g* and 4 °C for 20 min, and supernatants were submitted to phase partitioning at 37 °C for 5 min. Detergent-enriched and aqueous phases were then separated by centrifugation (5000 × *g*, 5 min). Each phase was washed twice; solutions were adjusted to 2% Triton X-114 and submitted to phase partitioning. Finally, each phase was adjusted to 1% Triton X-114 and immunoprecipitated overnight at 4 °C by anti-Bc28.1 rabbit serum.

Erythrocytes ghosts were obtained by freeze-thawing cycles followed by several washes of membranes with phosphate-buffered saline until hemoglobin had been removed. Ghosts were then boiled in SDS-PAGE reducing sample buffer.

Live Merozoite Preparation—Expression plasmid containing the coding sequence of equinatoxin II from *Actinia equina* (a kind gift from Dr. G. Anderluh, University of Ljubljana (Ljubljana, Slovenia)) was used to produce equinatoxin II in *Escherichia coli*. As described for *P. falciparum* (14), erythrocytes parasitized by *B. canis* were lysed by incubation with 150 μg/ml equinatoxin II in PBS. After several washes in PBS (centrifugation for 5 min at 1200 × *g*), merozoite samples were treated with anti-Bc28.1 rabbit serum for 30 min in PBS and then with FITC-conjugated anti-rabbit antibody (Sigma). With other samples of the same batch, merozoite viability was assessed by incubation with 6-carboxyfluorescein diacetate or propidium iodide. Live cells were then deposited between two microscopy slides and imaged with FITC, TRITC, and DAPI filter sets (Axioskop, Zeiss).

Western Blot and Immunofluorescence Analysis—After running in SDS-PAGE, the protein samples were transferred using semidry blotter onto nitrocellulose membranes, and membranes were then incubated for 1 h in blocking buffer (PBS, 0.1% Tween 20, 5% non-fat dry milk). Duplicate membranes were incubated for 1 h either with mAb 6C9 supernatant (1:500 in PBS, 0.1% Tween 20) or hybridoma culture medium at the same dilution, washed, and incubated with anti-mouse peroxidase-conjugated secondary antibody (Sigma). Chemiluminescent peroxidase substrate (West Pico supersignal substrate, Pierce) was added, and blots were analyzed using a Gnome CCD imager and GeneSnap software (Syngene).

For immunofluorescence analysis, parasitized red blood cells from an *in vitro* culture of *B. canis* A were washed in RPMI 1640 and fixed on Teflon-coated slides by acetone/methanol (4:1) at −20 °C. Slides were incubated for 1 h with mAb 6C9 culture supernatant serially diluted in PBS in a wet chamber, washed, and then incubated with FITC-conjugated anti-mouse antibody (Sigma) containing 10 μg/ml DAPI (Sigma), mounted with Citifluor, and observed with immersion oil (×100) on a fluorescence microscope with an FITC filter set (Axioskop, Zeiss). Images were captured with a digital camera fitted on the microscope.

Immunoprecipitation—B. canis parasites were metabolically labeled in the presence of [^{35}S]methionine, parasitized erythrocytes were washed three times in RPMI, and the packed cells were then lysed in 10 volumes of radioimmune precipitation buffer (10 mM Tris, 150 mM NaCl, 600 mM KCl, 5 mM EDTA, 2% Triton X-100, pH 7.8). After 1 h on ice, lysates were centrifuged at 16,000 × *g* for 20 min to remove insoluble materials. The soluble fraction (50 μl) or culture supernatant (200 μl) was then mixed with 5 μl of serum and incubated overnight at 4 °C under agitation. A volume of 50 μl of Protein A-Sepharose CL4B (GE Healthcare) equilibrated in radioimmune precipitation buffer (50% slurry) was then added and incubated for 1 h at room temperature under agitation. Beads were then washed three times in radioimmune precipitation buffer and boiled in SDS-PAGE sample buffer, and bound proteins were resolved on SDS-PAGE. After Coomassie staining, gels were dried in Amplify (GE Healthcare) and imaged using X-Omat films (Eastman Kodak Co.).

Erythrocyte Binding Assays—Dog erythrocytes (50 μl of packed cells) were washed three times with PBS and incubated with purified recombinant proteins (0.5 mg in 1 ml of PBS) for 1 h with rotations. Erythrocytes were then harvested by centrifugation (1800 × *g*, 3 min) and layered on silicon oil ($d = 1.05$, Sigma). After centrifugation (4000 × *g*, 3 min), supernatant and silicon oil were carefully removed, and bound proteins were eluted from erythrocytes using 50 μl of PBS containing 0.5 M NaCl. Experiments were done either with an increasing amount of erythrocytes (packed cell volume ranging from 10 to 100 μl) or an increasing amount of recombinant Bc28.1 protein (0.5, 1, and 1.5 mg in 1 ml of PBS). Unbound and bound proteins were then analyzed by Western blot using HRP-conjugated anti-His tag antibody (Qiagen) revealed with WestPico chemiluminescent substrate (Pierce).

Protein Expression and Purification—The sequence coding for the predicted full-length recombinant Bc28.1 polypeptide (see Fig. 1; accession number CS019629) from Ser^{18} to Asp^{235} was cloned in pIVEX 2.4a (Roche Applied Science), which appends a N-terminal hexahistidine tag using primers Bc28.1FLNterFor (5′-cgcttaattaaacatatgaccagctgcactgaggatgagaaaagggatagtgtc-3′) and Bc28.1FLRev (5′-ttagttagttaccggatcccttaatccttcttacccttggctccagatatac-3′), which both contain sequences complementary to the destination vector and to the Bc28.1 coding sequence to allow assembly by splicing of overlap extension. The forward primers Bc28delC19For (5′-cgcttaattaaacatatgaccactgaggatgagaaaagggatagtgtc-3′) and Bc28delA32For (5′-cgcttaattaaacatatgaccgctacgtccgttgaagccagcttaaag-3′) were used in association with Bc28.1FLRev to build the ΔC19-Bc28.1 and Δ-Bc28.1 recombinant proteins (see Fig. 2), respectively. The proofreading thermostable DNA polymerase Phusion (Finnzymes) was used for all amplification in cloning procedures. The recombinant vector was transformed in *E. coli* strain BL21(DE3) for protein production. Bacteria were cultivated in minimum M9-based medium containing NH_4Cl and glucose as the nitrogen and carbon source, respectively, isotopically enriched as needed (Eurisotop, St. Aubin, France). After cell growth and induction in an O_2-controlled fermentor operated in fed batch at 37 °C, cells were harvested and frozen at −80 °C. Cells were lysed in binding buffer (50 mM $NaPO_4$, 500 mM NaCl, 20 mM imidazole, pH 8.0) using a high pressure homogenizer at 1200 bars (Emulsiflex, Avestin). After the addition of polyethyleneimine (0.1%), centrifugation, and filtration, the clarified supernatant was loaded on a HisTrap column using AKTAExplorer, and the column was washed with 10 volumes of binding buffer contain-

ing 1 M NaCl and finally eluted in Tris 50 mM, pH 8.0, containing 400 mM imidazole. ^{15}N and $^{15}N/^{13}C$ and protein samples were concentrated to 0.5 mM and desalted in 10 mM sodium phosphate, 50 mM NaCl, 0.1 mM EDTA, pH 6.5.

Site-directed Mutagenesis—Based on the examination of the electrostatic properties of the Bc28.1 protein surface, mutagenesis was performed to disrupt the large positive area on one face of Bc28.1. The residues His^{128}, Arg^{129}, Lys^{137}, and Lys^{195} were changed either by glutamate or alanine using primers HRKalaRev (5′-agacaattccgccgcagtgatagaaagcacgtagag), HRKalaFor (5′-agccttaagaatgcgatcgatgaatggaag), K195alaFor (5′-gcggatatgatttacattaacgacgctatg), and K195Rev (5′gtgggacaccaattcgttaaccactgttgc) to construct the Bc28.1-HRKKAla mutant. The primers HRKgluFor (5′-agccttaagaatgaaatcgatgaatggaag), HRKgluRev (5′-agacaattcttcttcagtgatagaaagcacgtagag), K195gluFor (5′-gaagatatgatttacattaacgacgctatg), and K195Rev were used to construct the mutant Bc28.1HRKKGlu. Each primer was purified and phosphorylated at 5′ extremities (Sigma-Genosys). The plasmid coding for the full-length recombinant Bc28.1 protein was used as template. After a first round of amplification with a first primer couple, the plasmid template was digested by DpnI (10 units, 15 min at 37 °C before clean-up) (NucleoSpin Extract II, Macherey-Nagel). The PCR product was then self-ligated and transformed in DH5a. Clones containing mutated plasmids were then screened, and a second round of amplification was done with the second primer couple followed by the same procedure. After verification by sequencing, mutated plasmids coding for Bc28.1HRKKGlu and Bc28.1HRKKAla were transformed in BL21(DE3) for expression and purification. Before testing their adhesion properties, the structure integrity of the two mutants was checked using CD spectroscopy.

NMR Spectroscopy—NMR experiments were performed at 37 °C on Bruker AVANCE 500 (triple resonance) or 600 and 700 MHz (double resonance) spectrometers equipped with 5-mm *Z*-gradient ^{1}H-^{13}C-^{15}N cryogenic probes. Backbone and Cβ resonance assignments were made using standard HNCA, HNCACB, CBCA(CO)NH, HNCO, and HN(CA)CO experiments (15) performed on the ^{15}N,^{13}C-labeled Bc28.1 sample. HN and Hα assignments were confirmed using ^{1}H,^{15}N and ^{1}H,^{13}C NOESY-HSQC experiments (mixing time 100 ms) recorded on the ^{15}N- or ^{15}N,^{13}C-labeled samples, respectively. The analysis of the aromatic and methyl regions of the spectrum was considerably facilitated by the analysis of two-dimensional NOESY (and TOCSY) experiments recorded on a Bruker AVANCE 950 MHz (with cryoprobe) spectrometer on an unlabeled 0.1 mM protein sample dissolved in deuterated buffer. ^{1}H chemical shifts were directly referenced to the methyl resonance of DSS, whereas ^{13}C and ^{15}N chemical shifts were referenced indirectly to the absolute frequency ratios $^{15}N/^{1}H = 0.101329118$ and $^{13}C/^{1}H = 0.251449530$. All NMR spectra were processed with GIFA (16).

Heteronuclear $^{15}N\{^{1}H\}$ NOE experiments were recorded on the Bruker AVANCE 700 spectrometer. Proton saturation was achieved by application of high power 120° pulses spaced at 20-ms intervals for 3 s prior to the first pulse on ^{15}N (17). A relaxation delay equal to 6 s between each scan was used in order to obtain a complete relaxation of water magnetization and to reduce effects arising from amide proton exchange. Moreover, the two experiments with and without proton saturation were acquired in an interleaved manner, FID by FID.

Structural Modeling—The 2164 assigned NOE peaks were classified into five categories (very strong (≤2.4 Å), strong (≤2.8 Å), medium (≤3.6 Å), weak (≤4.4 Å), or very weak (≤4.8 Å)). This set was completed with 341 ϕ and ψ dihedral angle restraints taken out from TALOS predictions (18). The initial structures of Bc28 were calculated using the program CYANA (19). A total of 100 structures were calculated at this stage. The 20 best structures (based on the final target penalty function values) were minimized with CNS 1.2 according the RECOORD procedure (20) and analyzed with PROCHECK (21). The root mean square deviations were calculated with MOLMOL (22).

RESULTS

Sequence Comparison of Bc28.1, Bc28.2, and B. gibsoni Putative Orthologues—As previously described (10) and summarized here for clarity, Bc28.1 belongs to a multigenic family containing seven putative members, as assessed by DNA hybridization on pulsed field gel electrophoresis-separated restriction fragments. Currently, two members of this family have been identified in *B. canis*: Bc28.1, presented in this paper, and Bc28.2 (accession number CS019631). Large regions of these two proteins share a high level of identity, as shown by sequence alignment (Fig. 1). The C-terminal part of Bc28.2 is shorter and displays significant sequence variations with respect to Bc28.1. As described (10), the expression of Bc28.2 involves a translational frameshift mechanism without the introduction of a stop codon, so that the resulting Bc28.2 coding sequence is expressed as a 45-kDa protein. The description of the Bc28 family and the characterization of all members is still in progress. The current work focuses on the structural and functional analysis of Bc28.1 protein.

BLAST database mining using Bc28.1 sequence as a query detects a group of four different proteins in *B. gibsoni* (p32, p45, p47, and p50), another agent of canine babesiosis. All of these proteins were found in many strains of *B. gibsoni*. Alignment of Bc28.1 sequence with representative sequences of these four proteins (accession numbers gi258611174, gi148362039, gi284002400, and gi14646759, respectively) reveals significant homology (Fig. 1). As discussed further, structurally relevant residues are conserved in two main blocks separated by large insertions in the larger *B. gibsoni* proteins.

All of these proteins are putative GPI-anchored surface proteins, as suggested by the presence of the characteristic hydrophobic glycosylphosphatidylinositol signal at the C-terminal end of the sequence (residues 235–256 for Bc28.1) and the N-terminal signal peptide (residues 1–17) for endoplasmic reticulum targeting, mandatory for GPI-protein maturation. Supporting this assumption, in the case of Bc28.1, we demonstrate further that this protein is anchored at the surface of the merozoite.

Bc28.1 Protein Is Major Antigen in B. canis—Sequence analysis of the membrane protein Bc28.1 deduced from cDNA indicates the presence of an N-terminal signal peptide and a C-terminal hydrophobic GPI anchoring signal (Fig. 2). These

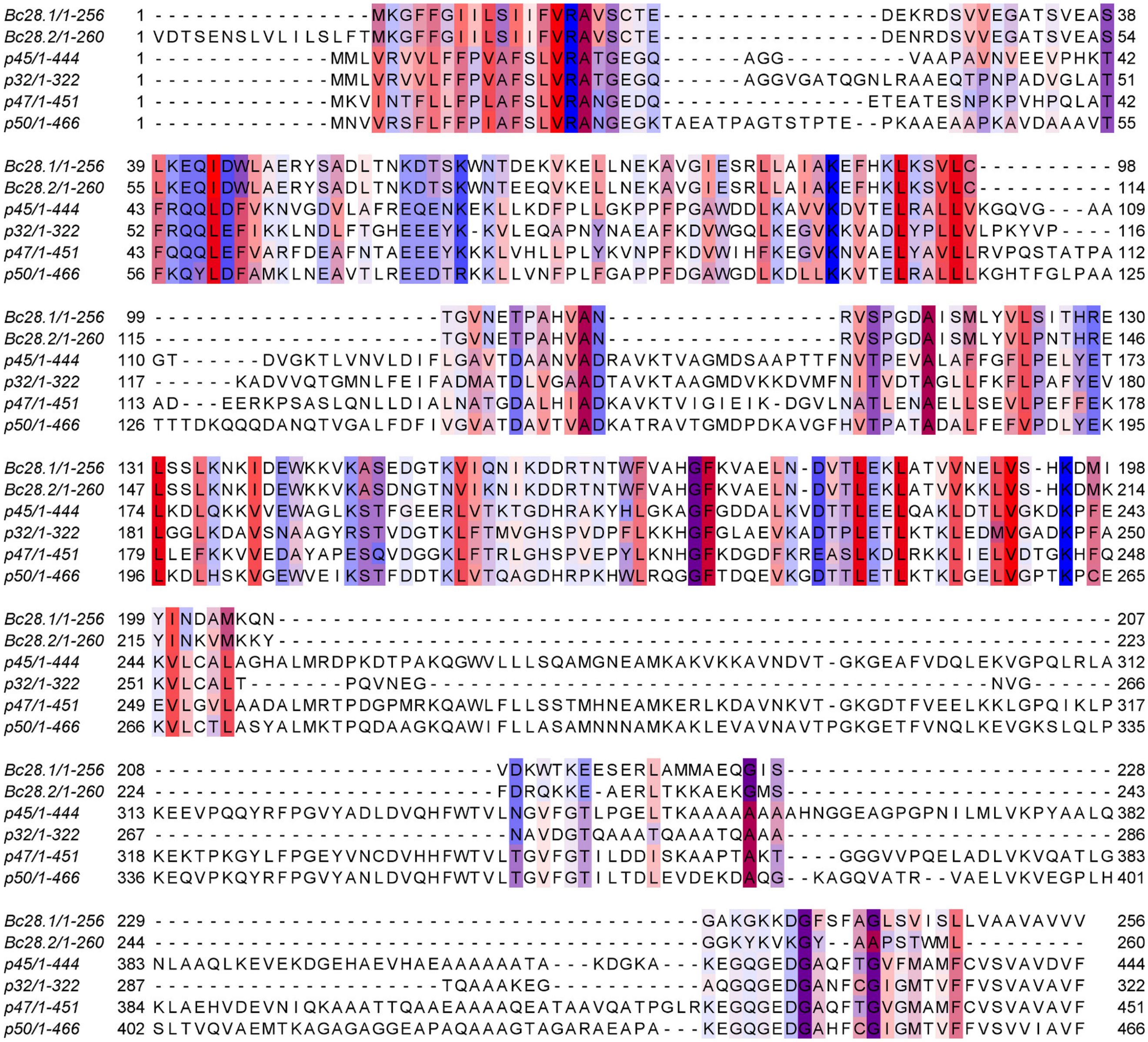

FIGURE 1. **Sequence alignment of Bc28.1 and Bc28.2 from *B. canis* with related proteins from *B. gibsoni* (p45, gi258611174; p32, gi148362039; p47, gi284002400; and p50, gi14646759).** Only residues above the 30% conservation threshold are *boxed*. The *color scheme* is for the hydrophobicity of residues (most hydrophobic in *red*, most hydrophylic in *blue*).

sequences are potentially removed during protein maturation in the parasite, with concomitant GPI addition. Also, the parasite produces a soluble form of Bc28.1 (see below). A recombinant protein corresponding to the full-length soluble mature protein was produced (His-Bc28.1; Fig. 2) and used for most of the further studies reported in this paper. Two other recombinant proteins were also produced (ΔC19-Bc28.1 and Δ-Bc28.1; Fig. 2) to further confirm the limits of the structured core of the protein. All of these constructs were expressed as soluble proteins in *E. coli*.

An equivalent amount of dog erythrocyte ghosts (parasitized or not) and recombinant proteins (Bc28.1 or His-GST) were loaded on SDS-PAGE (Fig. 3*A*) and analyzed by Western blot using the mAb 6C9 raised against merozoites of *B. canis* A. This antibody specifically recognizes recombinant Bc28.1 (Fig. 3*B*, *lanes 3* and *4*), whereas a strong single band of similar molecular weight is detected in ghosts from parasitized red blood cells (Fig. 3*B*, *lanes 1* and *2*).

Ghosts prepared from parasitized red blood cells contain both erythrocyte and merozoite membranes. Thus, the protein content of ghosts from dog erythrocytes differs in the presence of *B. canis* parasites. In the ghost sample prepared from dog parasitized blood, some red blood cell proteins seem to disappear (*e.g.* the 80 kDa band in Fig. 3*A*, *lane 1*), whereas a large number of proteins, potentially expressed by the parasite, around 25–30 kDa can be detected (Fig. 3*A*, *lane 2*). Although a difference in antibody recognition between native and recombinant Bc28.1, as well as the existence of different proteins in the same gel band, cannot be ruled out, the strong signal obtained with the monoclonal antibody against Bc28.1 on parasitized ghosts suggests the expression of a relatively large amount of this protein by parasites (Fig. 3*B*, *lanes 1* and *2*). The

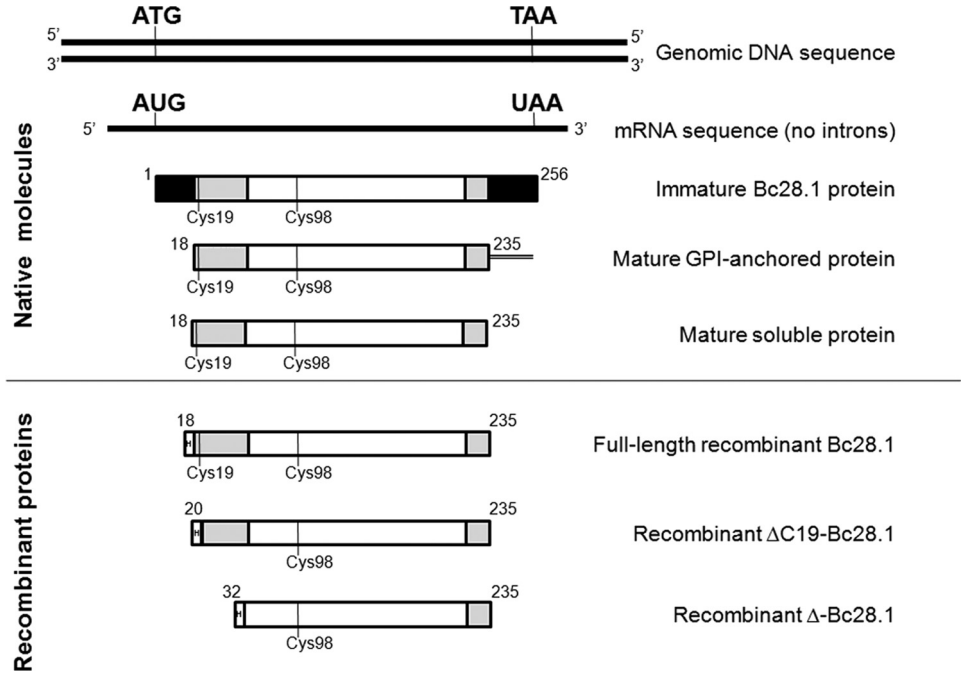

FIGURE 2. **Schematic description of the Bc28.1 sequence.** *Top*, molecules found in the parasite. The gene coding for Bc28.1 displays no intron, as evidenced by comparison of genomic and cDNA sequence. The Bc28.1 is translated as a precursor protein containing both N- and C-terminal hydrophobic sequences (*black boxes*) predicted to be a signal peptide and a GPI anchor signal, respectively. Mature GPI-anchored Bc28.1 was found at the merozoite surface, whereas a soluble form of the protein, potentially without a GPI anchor, was found produced inside the parasite and secreted in the *in vitro* culture supernatant. The three last sequences correspond to recombinant proteins used in the present study. In all sequence schemes, the structured core of the protein (Ser^{32}–Glu^{224}) is represented as *white boxes*, and unstructured parts (Ser^{18}–Ser^{38} and Glu^{224}–Asp^{235}) are shown as *gray boxes*.

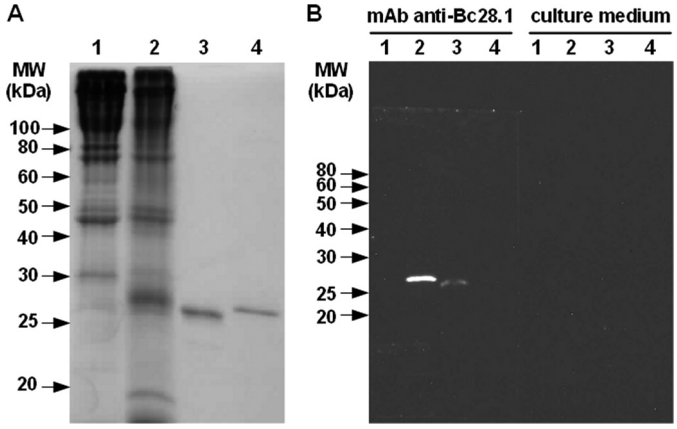

FIGURE 3. **Western blot detection of native and recombinant Bc28.1 protein by monoclonal antibody.** *A*, Coomassie-stained SDS-PAGE of the samples analyzed by Western blot. *B*, Western blots probed with hybridoma supernatant from monoclonal antibody 6C9 or with culture medium alone. *Lane 1*, ghosts from dog erythrocytes; *lane 2*, ghost from dog erythrocytes parasitized by *B. canis*; *lane 3*, recombinant Bc28.1 protein; *lane 4*, recombinant His-GST protein.

presence of this large amount of Bc28.1 in samples obtained from non-synchronized *in vitro* culture, suggests that Bc28.1 is one of the major proteins expressed by *B. canis* merozoites.

Bc28.1 Is Merozoite Surface Protein—The indirect immunofluorescence performed with rabbit serum against Bc28.1 (Fig. 4) shows the localization of this protein at the merozoite membrane. To assess the presence of Bc28.1 at the extracellular side of the merozoite membrane, immunofluorescence analyses were performed on live merozoites. Fluorescence labeling of merozoite with 6-carboxyfluorescein and the absence of propidium iodide inside cells indicate that merozoites are still alive after purification (a few dead merozoites can also be seen). The labeling of the live merozoite surface shows a heterogeneous repartition of Bc28.1, suggesting that regions of the merozoite surface do not contain this adhesion protein.

The Bc28.1 Protein Is Found in Supernatant of in Vitro Culture—Metabolic labeling of *B. canis* proteins with [^{35}S]methionine in cultures allows the sensitive detection of antigen specifically and natively recognized by antibodies. Immunoprecipitation, using polyclonal serum, from *in vitro* culture supernatants indicates the presence of Bc28.1 in such a fraction as a single band (Fig. 5*A*). Bc28.1 is a putative GPI-anchored protein, and the GPI anchor is known to be labile; hence, the presence of Bc28.1 in culture supernatants could result from constitutive release (*e.g.* by GPI-specific phospholipase) or shedding during invasion.

The use of a polyclonal antibody purified from anti-Bc28.1 rabbit serum using recombinant Bc28.1 allows us to increase the specific signal while reducing background. When this polyclonal antibody was used to immunoprecipitate culture supernatants, the same single band was found as with complete serum (Fig. 5*B*, *lane 1*). On the other hand, when the polyclonal antibody was used to immunoprecipitate extract prepared by Triton X-100 lysis of parasitized erythrocytes (total extract), two bands were found (Fig. 5*B*, *lane 2*). One of these bands corresponds to the protein found in culture supernatants (lower band of the doublet), whereas a slightly heavier protein is also present (higher band of the doublet). It is possible that the higher band corresponds to the membrane-anchored Bc28.1 protein and that the lower band corresponds to the membrane-released Bc28.1 protein.

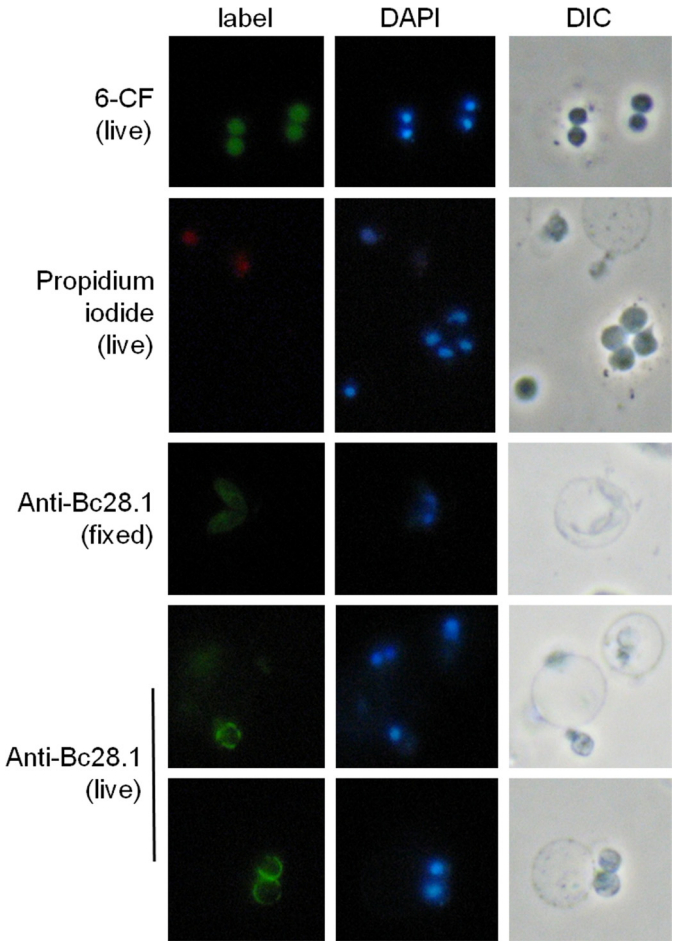

FIGURE 4. **localization of Bc28.1 at the *B. canis* merozoite surface by immunofluorescence on live cells.** Viability of *B. canis* merozoites assessed through fluorescent labeling with 6-carboxyfluorescein diacetate (*6-CF*) and the absence of propidium iodide labeling (two dead merozoites are positive in DAPI and propidium iodide, whereas five live merozoites are positive in DAPI and negative in propidium iodide). Rabbit anti-Bc28.1 serum was used to localize the protein on fixed merozoites (*middle*), showing a homogenous merozoite membrane pattern with internal structures labeled. On live merozoites (*bottom panels*), the observed pattern indicates the localization of Bc28.1 at the external side of the merozoite plasma membrane. Note the non-continuity of the labeling at the surface of merozoites. Control experiments with unrelated antibodies show no signal (data not shown). *DIC*, differential interference contrast.

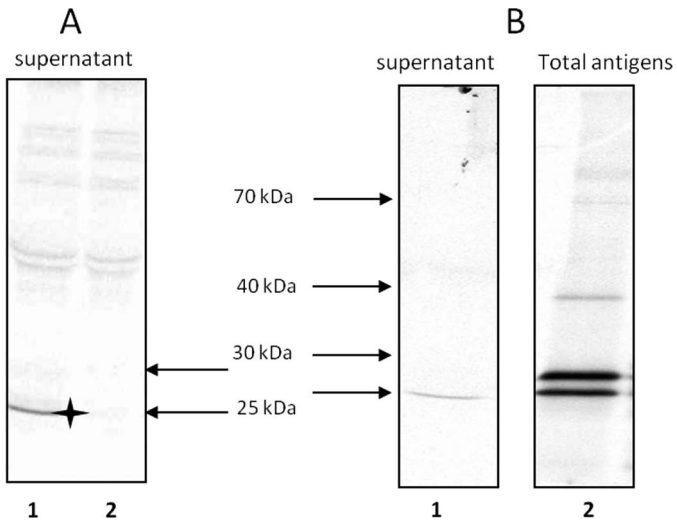

FIGURE 5. **Immunoprecipitation experiments performed with rabbit serum anti-Bc28.1 on supernatants or parasitic total extract from [^{35}S]methionine-labeled *B. canis* cultures.** *A*, culture supernatants immunoprecipitated with complete serum anti-Bc28.1 (*lane 1*) or preimmune serum (*lane 2*). The *star* indicates the band corresponding to Bc28.1 specifically immunoprecipitated. *B*, culture supernatants (*lane 1*) or total extract (*lane 2*) immunoprecipitated with purified rabbit polyclonal antibody anti-Bc28.1. Note the presence of two bands in the total extract.

To investigate the nature of the two bands found by immunoprecipitation in total extract, a protein fractionation based on their membrane properties was done. Immunoprecipitation was then performed on purified merozoites, parasitized erythrocyte ghosts, and the soluble fraction (Fig. 6*A*) using either anti-Bc28.1 or preimmune serum. The higher band of the doublet found in Triton X-100 extract was found both in purified merozoites and ghosts, strongly indicating a membrane association. The lower band was found in the soluble fraction resulting from hypotonic lysis during ghost preparation, suggesting the lack of a hydrophobic anchor in this molecule.

From this first fractionation step, purified merozoites and soluble fraction were each submitted to Triton X-114 phase partitioning (Fig. 6*B*). The results clearly show that the protein detected by the anti-Bc28.1 in purified merozoite serum is found in the detergent-enriched fraction. On the other hand, the protein detected in the soluble fraction (from hypotonic lysis) is found in the aqueous phase of Triton X-114 partitioning. These results indicate that from the two bands immunoprecipitated in total extract (Fig. 5*B*, *lane 2*), the lower band is found in the soluble fraction and represents a protein without an anchor. The higher band is found in fractions containing membranes or in detergent-enriched fractions and hence probably bears a GPI anchor.

Bc28.1 Is Erythrocyte-binding Protein—The merozoite surface localization of Bc28.1 protein suggests a role in the interaction with erythrocytes. The recombinant protein Bc28.1 was then tested for dog erythrocyte binding properties. As shown in Fig. 7, the protein was able to bind dog erythrocytes even if, as already described for the Bd37 protein from *B. divergens*, the amount of bound protein appears to be rather low in regard to the unbound quantity. When the amount of erythrocytes was increased, keeping constant the amount of Bc28.1, an increasing amount of bound Bc28.1 was recovered from the binding assay. Reciprocally, keeping constant the packed cell volume, an increasing amount of bound Bc28.1 was recovered when the amount of protein was increased in the binding assay. Even if the binding of recombinant Bc28.1 has not reached saturation, these results indicate that the low amount of bound Bc28.1 protein is not due to recombinant protein degradation or to erythrocyte denaturation.

In Vitro Growth Inhibition Assay—The effect of monoclonal antibody 6C9 at 1 mg/ml as well as 10% anti-Bc28.1 rabbit serum was assessed in the *in vitro* culture. Although Bc28.1 is located at the surface of merozoites and has an erythrocyte binding function, the presence of antibodies, either rabbit serum or monoclonal antibody, has no significant effect on the *in vitro* development of *B. canis* parasite (supplemental Fig. 1). In comparison and in agreement with previous studies (23), a 50% inhibition of the parasite development was obtained with

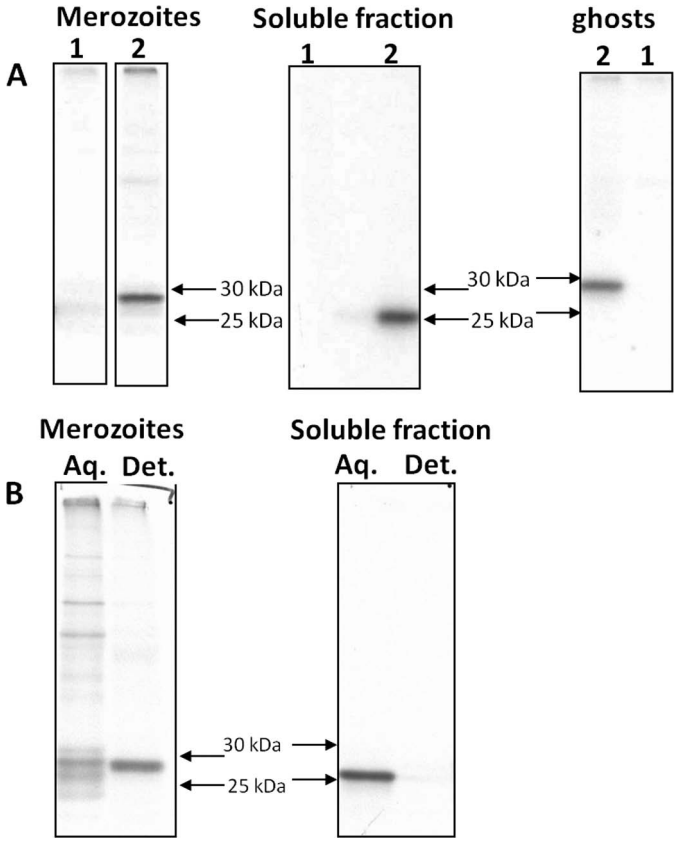

FIGURE 6. **membrane-bound and soluble forms of Bc28.1 immunoprecipitated from fractionated samples.** *A*, [^{35}S]methionine-labeled, parasitized dog erythrocytes were fractionated in purified merozoites, soluble fraction, and ghosts and then immunoprecipitated either with preimmune serum (*lanes 1*) or rabbit anti-Bc28.1 serum (*lanes 2*). *B*, purified merozoites and soluble fraction were submitted to Triton X-114 phase partitioning. The detergent-enriched phase (*Det.*) and aqueous phase (*Aq.*) were then immunoprecipitated using anti-Bc28.1 serum.

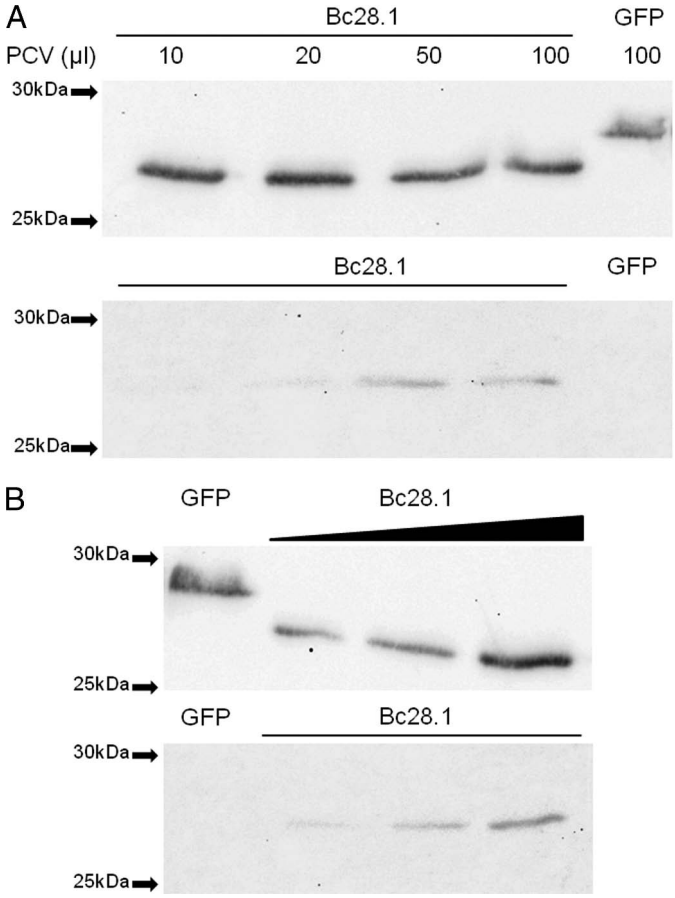

FIGURE 7. **Bc28.1 is an erythrocyte-binding protein from *B. canis*.** *A*, binding assay performed with increasing amounts of dog erythrocytes (*PCV*, packed cell volume ranging from 10 to 100 μl). His-GFP is used as a negative control. *Upper gel*, unbound proteins; *lower gel*, bound proteins revealed by anti-His tag. *B*, binding assay with increasing amounts of recombinant Bc28.1 and a constant amount (50 μl) of packed red blood cells. His-GFP is used as a negative control. *Upper gel*, unbound proteins; *lower gel*, bound proteins revealed by anti-His tag.

an immune serum directed against the intracellular viral BcVir15 protein and used as a positive control.

NMR Spectroscopy and Solution Structure—We produced and purified the recombinant Bc28.1 protein in ^{15}N-enriched medium in *E. coli* as described under "Experimental Procedures." The full-length construct Bc28.1 (Ser^{18}–Asp^{235}) corresponds to a soluble version of the parasite full-length membrane protein, missing the GPI anchor sequence and the N-terminal signal peptide, and still containing 2 cysteine residues (see Fig. 2). Its ^{1}H-^{15}N HSQC spectrum is shown in Fig. 8. By combining the information from ^{1}H-^{15}N double resonance and ^{1}H-^{15}N-^{13}C triple resonance heteronuclear experiments, we were able to assign more than 99% of the amide group resonances for the non-proline residues (2 prolines), 95.3% of the other backbone resonances (Cα, C′, and Hα), and more than 82% of the Cβ. TALOS analysis (18) of the (ϕ,ψ) intraresidual dihedral angles as well as the preliminary inspection of backbone-backbone NOEs show a predominant content of α-helical structure. As indicated by negative or weak values for heteronuclear ^{15}N{^{1}H} NOEs (supplemental Fig. 2), the N- and C-terminal peptide segments (Ser^{18}–Ser^{38} and Glu^{224}–Asp^{235}) appear highly disordered, with chemical shifts and (ϕ,ψ) values characteristic of a random coil structure. The chemical shifts have been deposited in the BioMagResBank under the accession number BMRB-17633.

CYANA structures were built from a restraint set consisting in 2164 NOE-derived restraints and 341 ϕ and ψ backbone dihedral angle restraints taken out from TALOS predictions. In addition, 33 χ_1 side chain dihedral angle restraints were used for residues for which Hβ proton stereospecific assignment can be made unambiguously. The 20 best structures (target penalty function values of $<$3.9 Å^2) were minimized with CNS 1.2 according to the RECOORD procedure (Fig. 9*A*). The resulting refined structures have no distance violation greater than 0.28 Å and no angular violation greater than 3.61°. When analyzed with PROCHECK, 88.9% of the residues fall in the most favored regions of the Ramachandran plot, and 9.8% are in the additional allowed regions. Only 0.9 and 0.4% of the residues fall in the generously allowed and disallowed regions, respectively. They correspond to residues located in the N-terminal disordered segment of the protein. Root mean square deviations of 1.15 and 1.77 Å were calculated with MOLMOL for backbone and all heavy atoms, respectively, in the structured part of the molecule (residues 24–200). Statistics are summarized in Table 1.

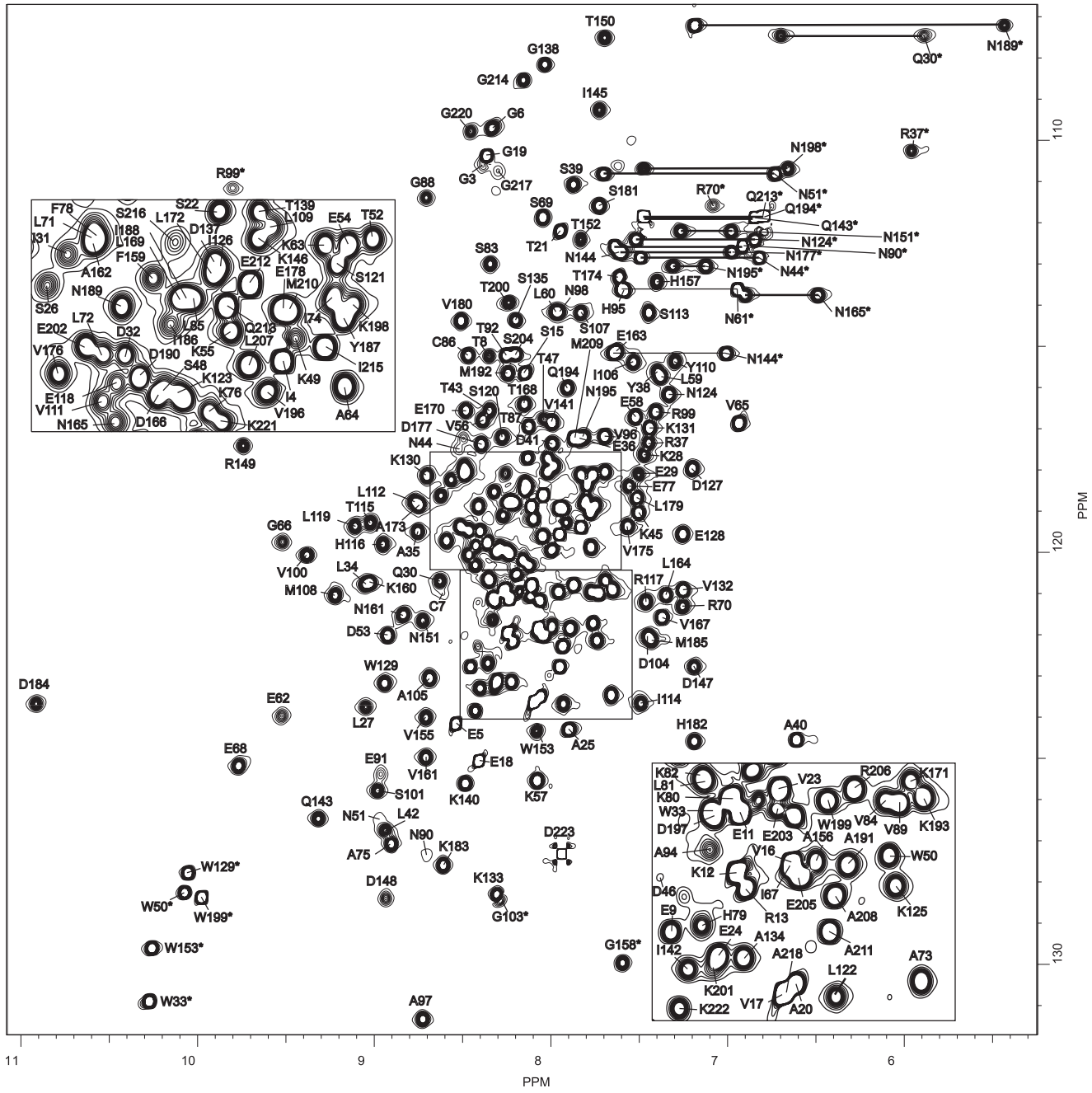

FIGURE 8. **Bc28.1 NMR fingerprint [^{1}H-^{15}N]HSQC spectrum of Bc28.1 from *B. canis* recorded at 700 MHz, 37 °C, and pH 6.5 on a 0.5 mM uniformly ^{15}N-labeled sample.** Cross-peak assignments are indicated using the one-letter amino acid and number (*stars* indicate HN indolic resonances from tryptophan residues). The central part of the spectrum is expanded in the two *insets*.

Bc28.1 presents a roughly ovoid shape with a main axis length and diameter of roughly 65 and 30 Å, respectively (Fig. 9*B*). Like Bd37, it falls into the category of the mainly α folds (24), consisting of seven antiparallel helices. However, the topology of the two proteins is markedly different (Fig. 9, *C* and *E*). In Bc28.1, these helices are arranged in a four-helix bundle with a non-canonical topology; two symmetrical motifs wrap around to form the bundle, burying the hydrophobic residues. Each motif consists of a long helix (helix 4 and 3, respectively), flanked on one side by two spatially contiguous shorter helices (helix 5 and 1 and helix 6 and 7). Although the length of helix 4 is comparable with the added lengths of the shorter helices 1 and 5, helix 3 is significantly shorter than the helical segment formed by helix 6 and 7; as a result, a large part of helix 7 protrudes from the bundle. Helix 2 closes one of the extremities of the bundle, whereas the other extremity is capped by the long loop joining helix 5 and 6. This organization is completely different from that observed for Bd37, where the helices are arranged in three subdomains (Fig. 9*D*), suggesting that these two proteins belong to distinct protein families. Research of fold analogues in the Protein Data Bank with DALI (25, 26) did not return any significant candidates, confirming that the α-helical bundle of Bc28.1 presents indeed a new topology.

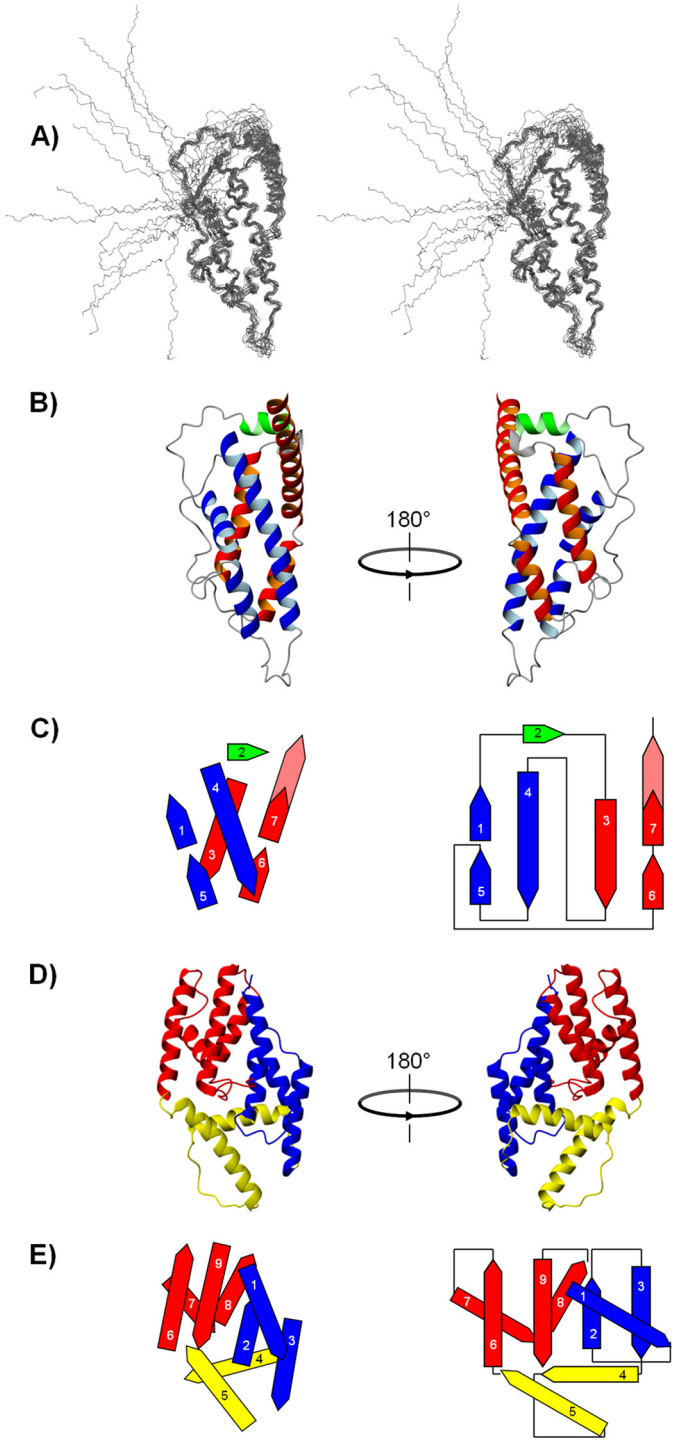

FIGURE 9. **Solution structure of Bc28.1 from *B. canis*; comparison with the three-dimensional structure and topology of Bd27 from *B. divergens*.** *A*, stereoview of an overlay of the 20 deposited NMR structures with lowest energy from CNS 1.2 calculation. *B*, two 180° rotated views of Bc28.1 (*ribbon representation*) showing the arrangement of the two symmetrical motifs involved in the α-helical bundle. The long helix 4 and the two short helices 1 and 5 form the first motif (in *blue*), whereas the second motif (in *red*) consists of the long helix 3, the short helix 6, and the N-terminal part of helix 7. *C*, topological diagram (*right*) and side view projection (*left*) of the spatial arrangement of the helices in the α-helical bundle. The same *color code* has been used as in *B* except for the solvent-exposed section of helix 7, which is *colored* in *dashed red*. *D*, two 180° rotated views of ΔBd37 (*ribbon representation*). The N- and C-terminal subdomains are *colored* in *blue* and *red*, respectively, and the putative hinge region is *yellow* (for details, see Ref. 12). *E*, topological diagram (*right*) and side view projection (*left*) of the spatial arrangement of the helices in the three-dimensional structure of ΔBd37 (same *color code* as for the *ribbon representation*).

TABLE 1
Statistics for the calculations of the solution structure of Bc28.1
Root mean square deviations were calculated over mean coordinates by MOLMOL.

Parameters	Values
NMR distance and dihedral constraints	
Distance constraints	
Total NOE	2164
Intraresidue	540
Interresidue	
Sequential ($\|i-j\|=1$)	737
Medium-range ($\|i-j\|<4$)	540
Long-range ($\|i-j\|>5$)	347
Intermolecular	
Total dihedral angle restraints	
ϕ	171
ψ	170
χ_1	33
Structure statistics	
Violations (mean ± S.D.)	
Maximum distance constraint violation (Å)	0.18 ± 0.04
Maximum dihedral angle violation (degrees)	2.53 ± 0.51
Deviations from idealized geometry	
Bond lengths (Å)	0.010 ± 0.001
Bond angles (degrees)	1.200 ± 0.024
Impropers (degrees)	1.423 ± 0.050
Ramachandran plot (%)	
Most favored region	88.9
Additionally allowed region	9.8
Generously allowed region	0.9
Disallowed region	0.4
Average pairwise root mean square deviation (Å) (backbone/heavy)	
Residues 24–200	1.15 ± 0.20/1.77 ± 0.23

As found for Bd37, the major GPI-anchored adhesion protein from *B. divergens*, the N-terminal (as well as the 10 last C-terminal residues) segment (Ser^{18}–Ser^{38}) is disordered and bears a cysteine residue (Cys^{19}). However, contrary to Bd37, this cysteine residue is not disulfide-bridged with Cys^{98}, another cysteine present in the Bc28.1 sequence, buried in the hydrophobic core of the bundle. Indeed, although Cys^{98} cannot be assigned unambiguously, the chemical shift measured for the Cβ of Cys^{98} (30.14 ppm) corresponds to a carbon bearing a thiol function and does not exhibit the characteristic upfield shift of carbon involved in a disulfide bridge. In addition, no significant changes were observed for the core residues on an HSQC spectrum recorded on truncated constructs of Bc28.1 (ΔC19-Bc28.1 and Δ-Bc28.1; see Fig. 1) (not shown).

The surface of Bc28.1 is highly polar; one face of the molecule is highly basic, whereas the charge distribution on the opposite face is not so clearly defined (Fig. 10*A*). This is also clearly different from what was observed for Bd37, where electrostatic surface calculation reveals that the protein is largely negatively charged at physiological pH, with the exception of two negative patches (Fig. 10*B*).

Site-directed Mutagenesis Analysis—Because one of the basic patches at the surface of Bd37 has been proposed as being directly involved in the interaction with the negatively charged erythrocyte membranes (12), it is tempting to propose that the large basic patch at the surface of Bc28.1 could play a similar role in the adhesion process. To test this hypothesis, we have mutated the 4 residues that mainly account for the positive charge of this basic patch, namely His^{116}, Arg^{117}, Lys^{125}, and Lys^{183} (Fig. 10*A*). Note that other basic residues potentially contributing to this basic patch were not mutated because they are engaged in salt bridges with acidic residues in the NMR three-dimensional structure and probably contribute also to

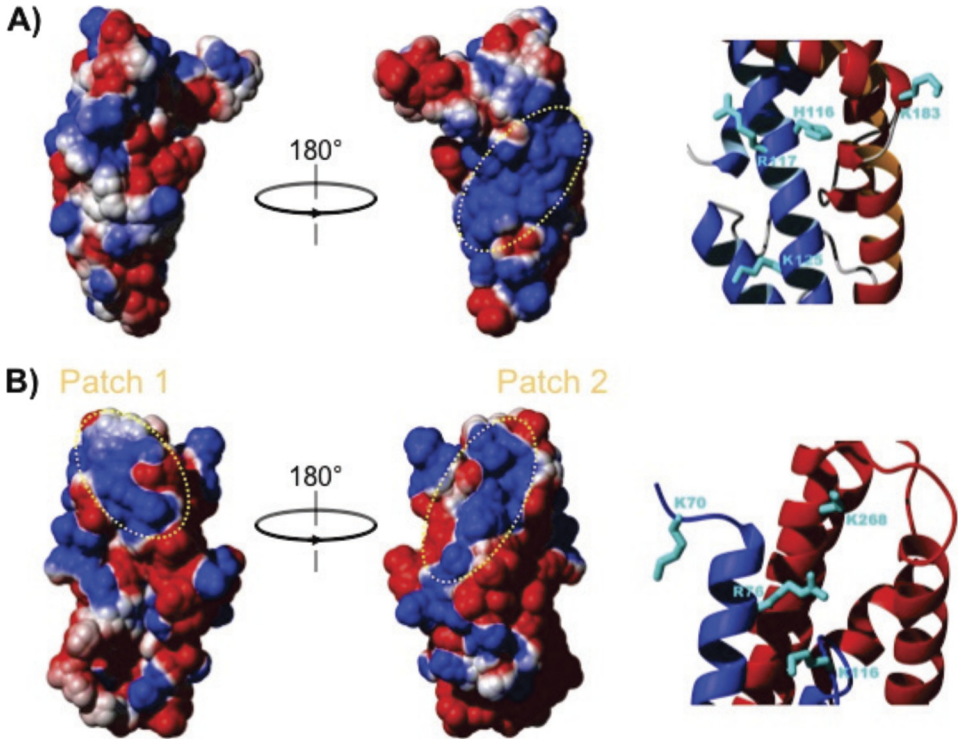

FIGURE 10. **Comparison of the electrostatic surface of Bc28.1 and Bd37.** *A*, two 180° rotated views of the electrostatic surface potential of Bc28.1 calculated using MOLMOL (21), with parameters chosen to represent physiological conditions. Electrostatic potential is represented as a tricolor gradient going from *blue* (+1 *kT*) over *white* (neutral) to red (−1 *kT*). The *dotted yellow ellipse* indicates the basic patch on one face of the protein structure. Basic residues accounting for the positive charge of this patch are reported on a *zoom* in the *ribbon representation*. *B*, two 180° rotated views of the electrostatic surface potential of Bd37 calculated using MOLMOL, with parameters as in *A*. Two basic patches appear clearly at the *top* of the molecule (*dotted yellow ellipses*). In the *rightmost structure*, the basic patch corresponds to the epitope of the monoclonal protective antibody mAb F4.2F8-INT. Basic residues accounting for the positive charge of this later patch are reported on a *zoom* in the *ribbon representation*.

protein stability. The selected residues were replaced either by alanine (Bc28.1_HRKKAla mutant), yielding a large hydrophobic surface, or glutamic residues (Bc28.1_HRKKGlu mutant), reversing the polarity of the corresponding surface (supplemental Fig. 3*A*). Mutant proteins were expressed in *E. coli* and purified as soluble proteins. The recombinant mutant proteins were then tested for dog erythrocyte binding properties. As shown in supplemental Fig. 3, the two proteins were still able to bind dog erythrocytes. This negative result suggests that the residues mutated on the basic patch at the surface of the wild-type protein are not sufficient to mediate the interaction with the erythrocyte membrane, although they could still contribute.

DISCUSSION

Bc28.1 was described here as a major protein from the *B. canis* merozoite surface. Immunofluorescence experiments show the localization of this protein at the merozoite membrane in late stages but also in young stages, although the expression time course of such molecules was not established. The presence of the protein anchored at the membrane of young parasites appears to be a common feature in Apicomplexa. The origin of these proteins, as newly synthesized molecules or proteins expressed prior to invasion, has rarely been investigated. In *B. divergens*, the Bd37 protein was found in young parasites inside human erythrocytes, but the protein's fate during invasion and its expression at an earlier stage was not determined. In one of the most studied cases, MSP1 in *P. falciparum*, the C-terminal GPI-anchored part of the complex is brought with the parasite during invasion, whereas other parts of the complex are shed from the membrane (27). Moreover, *P. falciparum* MSP-8, another GPI-anchored protein, has been shown to interact with parasitophorus and the food vacuole inside the erythrocyte (35, 28). Thus, GPI-anchored protein at the surface of young *Babesia* merozoites could also participate in potential interactions with host proteins inside the erythrocyte. The difference in ionic environment between extracellular medium and erythrocyte cytoplasm could induce such a switch in interaction partners. In the particular case of Bc28.1, as for many other GPI-anchored proteins in *Babesia*, the origin and functions of proteins found in young parasites remain to be elucidated.

The recombinant protein Bc28.1 was found to bind dog erythrocytes. Comparison with erythrocyte binding properties of other Apicomplexa proteins remains difficult, due to the lack of knowledge about these molecules. In fact, most of the studies performed with full-length proteins were based on gel analysis of bound and unbound proteins, using recombinant proteins or native proteins from *in vitro* culture supernatants. Such a binding assay was used, for instance, to characterize interactions between BAEBL, MSP1, and other proteins from *P. falciparum* and the red blood cell surface (29). Quantitative information, such as dissociation constants, has been obtained using peptides derived from *P. falciparum* proteins (30). Further exploration of the dynamics of Bc28.1 interaction with erythrocytes,

as well as identification of the receptor, will solve many outstanding questions concerning the invasion process. In particular, the first contact between the Apicomplexa parasite and the host cell relies on rapidly reversible interactions between such GPI-anchored proteins and the surface of the red blood cell (31). Such highly dynamic interactions could explain the small amount of bound Bc28.1 found in the erythrocyte binding tests as well as the difficulty of reaching saturation of erythrocytes.

Bc28.1 was found as well, as a soluble protein in the *in vitro* culture supernatant and in the parasite extract. Indeed, Triton X-114 phase partitioning strongly suggests that the two bands found in the immunoprecipitation of the extract prepared by Triton X-100 lysis of parasitized erythrocytes with polyclonal rabbit antibody correspond to a membrane-bound and a membrane-free form of the protein. This is a general feature of GPI-anchored merozoite membrane proteins from *Babesia* to be found either in culture supernatants or in the plasma of infected animals, but the mechanism leading to the absence of anchor is currently unknown. It could be related to proteolytic processing, degradation, phospholipase cleavage of GPI-anchored protein, or the synthesis of an unanchored protein, as suggested elsewhere (10). This could be also potentially due to an unbalanced enzymatic pathway in GPI synthesis, impacting the GPI anchor transfer to proteins. This abundant release of soluble antigens could represent the basis of an immune escape mechanism; large amounts of soluble antigens could overwhelm the host antibody production. Apicomplexa parasites (*e.g. B. bovis*) have been demonstrated to produce a high level of protein-free GPI that could interfere with the immune response against parasites (32, 36).

Antigens found in culture supernatant from *B. canis* are the basis of current vaccines against canine babesiosis (33, 34). However, the exact role of Bc28.1 in the protective immune response raised by such vaccines remains to be determined. As an erythrocyte-binding protein, Bc28.1 is involved in a key process for parasite development. Thus, we can hypothesize that an immune response targeting such a protein would have some protective abilities against parasite infection.

The effect of antibodies on the *in vitro* development of *B. canis* was determined using either rabbit serum anti-Bc28.1 or the mAb 6C9. Neither rabbit serum (up to 10% in the culture medium) nor mAb (up to 1 mg/ml in the culture medium) yield inhibition of *in vitro* growth of the parasites. There is not a strong correlation between the *in vitro* effect on parasite growth and the *in vivo* protective effect of antibodies. Indeed, if the GPI-anchored antigen MSA-1 from *B. bovis* is able to elicit antibodies that neutralize invasion *in vitro*, immunization of cattle with recombinant protein has failed to induce protection of animals (37). Conversely, the *in vivo* protective mAb F4.2F8 was not able to inhibit the *in vitro* growth of *B. divergens* parasites. The fact that antibodies directed against Bc28.1 do not inhibit the *in vitro* growth of *B. canis* could be related to many parameters. Among them, the antigen-antibody stoichiometry could be important as well as the amount of soluble Bc28.1 released by parasites that could bind a large part of the antibodies, leaving few antibodies free to neutralize the Bc28.1 fraction anchored at the parasite surface. Importantly, a similar massive release of soluble Bd37 protein was observed for *B. divergens*, without preventing the *in vivo* protective effect of the recombinant vaccine (11). In these cases, the incapacity of antibodies to inhibit *in vitro* parasite growth inhibition is not in contradiction with a putative role of the antigen in the invasion process. On the other hand, there are several examples where efficient *in vitro* growth inhibition by a neutralizing antibody cannot be correlated with a direct involvement of the antigen in the invasion process. This could be the case for anti-BcVir5 used as a positive control in the present study, directed against an intracellular viral protein whose role in the invasion process is still not clear and under debate. This is definitely the case for the monoclonal antibody DG7 directed against a heat shock protein from *B. divergens* that was shown to be able to inhibit the *in vitro* growth of the parasite but failed to protect animals (35). Finally, other effectors of the immune response are absent in an *in vitro* assay and could have a great incidence on the protection conferred by antibodies. Currently, a better assay to determine the protective potential of an antigen will be the immunization of animals and their subsequent challenge with infectious parasites. In this case, all of the components of the immune system will be involved together with antibodies in the response against parasites.

The solution structure of Bc28.1 is markedly different from the solution structure of Bd37 (12), an antigenic surface adhesion protein thought to play a similar role in *B. divergens*. The surface of Bc28.1 is highly polar, with one face being highly basic, whereas the charge distribution on the opposite face is not so clearly defined. Bd37 displays a largely negatively charged surface at physiological pH, with the exception of two basic patches, one of them roughly matching the epitope recognized by the neutralizing monoclonal antibody F4.2F8-INT (Fig. 10). Although monoclonal antibody epitopes are not presently mapped against Bc28.1, it was tempting to suggest that the basic face of the bundle might be involved, at least in an early, nonspecific stage, in the interaction with the negatively charged membrane of the erythrocyte. As proposed for Bd37, this positive surface might play a major role in the prior correct orientation and in the further binding of Bc28.1 to its putative receptor at the red blood cell membrane. Surprisingly, the two Bc28.1 mutants, in which positively charged amino acids in the basic patch were replaced either by alanine or glutamic acid, are still able to bind dog erythrocytes. It seems that, in addition to having unrelated three-dimensional structures and despite a similar function, the molecular mechanism of the interaction with the erythrocyte membrane could be different for Bd37 and Bc28.1. Possibly, these two merozoite surface proteins interact with different molecules outside the host cells. Also, it should be noted that we have only indirect evidence for the contribution of this basic patch at the surface of Bd37 to the adhesion process: the fact that it matches the epitope recognized by the neutralizing monoclonal antibody F4.2F8-INT. Because this protein is supposed to undergo an important conformational change during its adhesion to the red cell membrane, the neutralizing effect of F4.2F8-INT might challenge this mechanism rather than simply hide a potential interaction surface.

Interestingly, both proteins display a large unstructured solvent-exposed N-terminal region. The N terminus of Bd37 was

identified previously as highly polymorphic between different isolates of the parasite. The presence of a large unstructured and polymorphic region, which acts as an immunogenic lure attracting antibodies, probably represents a part of the immune escape mechanism of *B. divergens*. Such a strategy seems common to Apicomplexa because unstructured regions have been found in many apicomplexan proteins (3). In the case of Bc28.1, the polymorphism between different isolates of *B. canis* was found to be relatively low (96% amino acid identity) compared with the polymorphism of Bd37 between different isolates of *B. divergens* (ranging from 53 to 88% amino acid identity) (10). The reduced polymorphism of Bc28.1 in *B. canis*, compared with Bd37 in *B. divergens*, could reflect a weaker immune selective pressure on Bc28.1 than on Bd37. In contrast, this reduced polymorphism could reflect a more intense functional restraint for erythrocyte binding, impairing diversification of the Bc28.1 alleles. Further studies are needed to explore the exact role of such unstructured regions in both *Babesia* species, in particular their quantitative importance in immune escape mechanisms.

Although a DALI search for fold analogues in the Protein Data Bank did not return any significant candidates, a PSI-BLAST analysis performed with the Bc28.1 sequence as a query detected sequence homologies with four proteins of *B. gibsoni*, another agent of canine babesiosis. These proteins, including the p50 merozoite surface protein (36), are all putatively GPI-anchored at the merozoite membrane. The Clustal alignment of these four sequences with Bc28.1 reveals two major insertions in the *B. gibsoni* sequences compared with the one of *B. canis* (Fig. 1). These insertions of about 60 and 150 residues concern a loosely structured region in the Bc28.1 structure and should allow a global conservation of the three-dimensional structure in the *B. gibsoni* proteins. In addition, most of the hydrophobic residues are conserved between the four *B. gibsoni* sequences and Bc28.1, suggesting, at least, a partial conservation of the three-dimensional structure. The function of these orthologues from *B. gibsoni* is still unknown. Their homology with Bc28 suggests an erythrocyte binding ability, although no direct evidence has been reported. The use of the p50 recombinant protein in ELISAs revealed the presence of antibodies against this protein in dogs from the field (38). In addition, antibodies against recombinant p50 have been shown to inhibit the parasite development in a mouse model (39), and dog vaccination with both DNA coding for p50 and recombinant virus expressing p50 induces a weak protection against *B. gibsoni* parasites (40). Taken together, these results suggest that Bc28.1 from *B. canis* might also be targeted by host antibodies and then have some potential as a vaccine candidate.

CONCLUSIONS

The high sequence heterogeneity in these parasite-specific proteins impairs efficient domain definition using sequence homology. The structural analysis of at least one member in each family of GPI-anchored proteins in the Apicomplexa genus will provide new points of comparison between such parasites, allowing enhancement of the annotation of the parasitic genome and revealing new concepts in host-parasite molecular relationships. The resolution of the structure of Bc28.1 will provide as well a basis for functional analysis, in order to characterize the dual aspect of host interactions, namely erythrocyte binding and immune system interactions. Further studies are needed to better understand the interaction of this protein with the dog immune system.

REFERENCES

1. Irwin, P. J. (2009) Canine babesiosis. From molecular taxonomy to control. *Parasit. Vectors* **26,** Suppl. 1, S4
2. Fowkes, F. J., Richards, J. S., Simpson, J. A., and Beeson, J. G. (2010) The relationship between anti-merozoite antibodies and incidence of *Plasmodium falciparum* malaria. A systematic review and meta-analysis. *PLoS Med.* **7,** e1000218
3. Anantharaman, V., Iyer, L. M., Balaji, S., and Aravind, L. (2007) Adhesion molecules and other secreted host-interaction determinants in Apicomplexa. Insights from comparative genomics. *Int. Rev. Cytol.* **262,** 1–74
4. von Itzstein, M., Plebanski, M., Cooke, B. M., and Coppel, R. L. (2008) Hot, sweet and sticky. The glycobiology of *Plasmodium falciparum*. *Trends Parasitol.* **24,** 210–218
5. Ferguson, M. A. (1999) The structure, biosynthesis, and functions of glycosylphosphatidylinositol anchors and the contributions of trypanosome research. *J. Cell Sci.* **112**, 2799–2809
6. Brayton, K. A., Lau, A. O., Herndon, D. R., Hannick, L., Kappmeyer, L. S., Berens, S. J., Bidwell, S. L., Brown, W. C., Crabtree, J., Fadrosh, D., Feldblum, T., Forberger, H. A., Haas, B. J., Howell, J. M., Khouri, H., Koo, H., Mann, D. J., Norimine, J., Paulsen, I. T., Radune, D., Ren, Q., Smith, R. K., Jr., Suarez, C. E., White, O., Wortman, J. R., Knowles, D. P., Jr., McElwain, T. F., and Nene, V. M. (2007) Genome sequence of *Babesia bovis* and comparative analysis of apicomplexan hemoprotozoa. *PLoS Pathog.* **3,** 1401–1413
7. Jung, C, Lee, C. Y., and Grigg, M. E. (2004) The SRS superfamily of *Toxoplasma* surface proteins. *Int. J. Parasitol.* **34,** 285–296
8. Pollard, A. M., Onatolu, K. N., Hiller, L., Haldar, K., and Knoll, L. J. (2008) Highly polymorphic family of glycosylphosphatidylinositol-anchored surface antigens with evidence of developmental regulation in *Toxoplasma gondii*. *Infect. Immun.* **76,** 103–110
9. Gilson, P. R., Nebl, T., Vukcevic, D., Moritz, R. L., Sargeant, T., Speed, T. P., Schofield, L., and Crabb, B. S. (2006) Identification and stoichiometry of glycosylphosphatidylinositol-anchored membrane proteins of the human malaria parasite *Plasmodium falciparum*. *Mol. Cell. Proteomics* **5,** 1286–1299
10. Carcy, B., Précigout, E., Schetters, T., and Gorenflot, A. (2006) Genetic basis for GPI-anchor merozoite surface antigen polymorphism of *Babesia* and resulting antigenic diversity. *Vet. Parasitol.* **138,** 33–49
11. Delbecq, S., Hadj-Kaddour, K., Randazzo, S., Kleuskens, J., Schetters, T., Gorenflot, A., and Précigout, E. (2006) Hydrophobic moieties in recombinant proteins are crucial to generate efficient saponin-based vaccine against Apicomplexan *Babesia divergens*. *Vaccine* **24,** 613–621
12. Delbecq, S., Auguin, D., Yang, Y. S., Löhr, F., Arold, S., Schetters, T., Précigout, E., Gorenflot, A., and Roumestand, C. (2008) The solution structure of the adhesion protein Bd37 from *Babesia divergens* reveals structural homology with eukaryotic proteins involved in membrane trafficking. *J. Mol. Biol.* **375,** 409–424
13. Bordier, C. (1981) Phase separation of integral membrane proteins in Triton X-114 solution. *J. Biol. Chem.* **256,** 1604–1607
14. Jackson, K. E., Spielmann, T., Hanssen, E., Adisa, A., Separovic, F., Dixon, M. W., Trenholme, K. R., Hawthorne, P. L., Gardiner, D. L., Gilberger, T., and Tilley, L. (2007) Selective permeabilization of the host cell membrane of *Plasmodium falciparum*-infected red blood cells with streptolysin O and equinatoxin II. *Biochem. J.* **403,** 167–175
15. Sattler, M., Schleucher, J., and Griesinger, C. (1999) *Prog. NMR Spec.* **34,** 93–158
16. Pons, J. L., Malliavin, T. E., and Delsuc, M. A. (1996) Gifa version 4. A complete package for NMR data set processing. *J. Biomol. NMR* **8,** 445–452
17. Kay, L. E., Torchia, D. A., and Bax, A. (1989) Backbone dynamics of proteins as studied by ^{15}N inverse detected heteronuclear NMR spectroscopy. Application to staphylococcal nuclease. *Biochemistry* **28,** 8972–8979

18. Cornilescu, G., Delaglio, F., and Bax, A. (1999) Protein backbone angle restraints from searching a database for chemical shift and sequence homology. *J. Biomol. NMR* **13,** 289–302
19. Güntert, P. (2004) Automated NMR structure calculation with CYANA. *Methods Mol. Biol.* **278,** 353–378
20. Nederveen, A. J., Doreleijers, J. F., Vranken, W., Miller, Z., Spronk, C. A., Nabuurs, S. B., Güntert, P., Livny, M., Markley, J. L., Nilges, M., Ulrich, E. L., Kaptein, R., and Bonvin, A. M. (2005) RECOORD. A recalculated coordinate database of 500+ proteins from the PDB using restraints from the BioMagResBank. *Proteins* **59,** 662–672
21. Laskowski, R. A., Rullmannn, J. A., MacArthur, M. W., Kaptein, R., and Thornton, J. M. (1996) AQUA and PROCHECK-NMR. Programs for checking the quality of protein structures solved by NMR. *J. Biomol. NMR* **8,** 477–486
22. Koradi, R., Billeter, M., and Wüthrich, K. (1996) MOLMOL. A program for display and analysis of macromolecular structures. *J. Mol. Graph.* **14,** 51–55
23. Drakulovski, P., Carcy, B., Moubri, K., Carret, C., Depoix, D., Schetters, T. P., and Gorenflot, A. (2003) Antibodies raised against Bcvir15, an extrachromosomal double-stranded RNA-encoded protein from *Babesia canis*, inhibit the *in vitro* growth of the parasite. *Infect. Immun.* **71,** 1056–1067
24. Orengo, C. A., Michie, A. D., Jones, S., Jones, D. T., Swindells, M. B., and Thornton, J. M. (1997) CATH. A hierarchic classification of protein domain structures. *Structure* **5,** 1093–1108
25. Holm, L., and Sander, C. (1999) Protein folds and families. Sequence and structure alignments. *Nucleic Acids Res.* **27,** 244–247
26. Holm, L., and Rosenström, P. (2010) Dali server. Conservation mapping in 3D. *Nucleic Acids Res.* **38,** W545–W549
27. Blackman, M. J., Heidrich, H. G., Donachie, S., McBride, J. S., and Holder, A. A. (1990) A single fragment of a malaria merozoite surface protein remains on the parasite during red cell invasion and is the target of invasion-inhibiting antibodies. *J. Exp. Med.* **172,** 379–382
28. Drew, D. R., Sanders, P. R., and Crabb, B. S. (2005) *Infect. Immun.* **7,** 3912–3922
29. Boyle, M. J., Richards, J. S., Gilson, P. R., Chai, W., and Beeson, J. G. (2010) Interactions with heparin-like molecules during erythrocyte invasion by *Plasmodium falciparum* merozoites. *Blood* **115,** 4559–4568
30. García, J., Curtidor, H., Pinzón, C. G., Vanegas, M., Moreno, A., and Patarroyo, M. E. (2009) Identification of conserved erythrocyte binding regions in members of the *Plasmodium falciparum* Cys6 lipid raft-associated protein family. *Vaccine* **27,** 3953–3962
31. Bannister, L. H., and Dluzewski, A. R. (1990) The ultrastructure of red cell invasion in malaria infections. A review. *Blood Cells* **16,** 257–292; discussion 293–297
32. Rodríguez, A. E., Couto, A., Echaide, I., Schnittger, L., and Florin-Christensen, M. (2010) *Babesia bovis* contains an abundant parasite-specific protein-free glycerophosphatidylinositol and the genes predicted for its assembly. *Vet. Parasitol.* **167,** 227–235
33. Schetters, T. P., Moubri, K., and Cooke, B. M. (2009) Comparison of *Babesia rossi* and *Babesia canis* isolates with emphasis on effects of vaccination with soluble parasite antigens. A review. *J. S. Afr. Vet. Assoc* **80,** 75–78
34. Moreau, Y., Vidor, E., Bissuel, G., and Dubreuil, N. (1989) Vaccination against canine babesiosis. An overview of field observations. *Trans. R. Soc. Trop. Med. Hyg.* **83,** (suppl.) 95–96
35. Precigout, E., Delbecq, S., Vallet, A., Carcy, B., Camillieri, S., Hadj-Kaddour, K., Kleuskens, J., Schetters, T., and Gorenflot, A. (2004) Association between sequence polymorphism in an epitope of *Babesia divergens* Bd37 exoantigen and protection induced by passive transfer. *Int. J. Parasitol.* **34,** 585–593
36. Fukumoto, S., Xuan, X., Nishikawa, Y., Inoue, N., Igarashi, I., Nagasawa, H., Fujisaki, K., and Mikami, T. (2001) Identification and expression of a 50-kilodalton surface antigen of *Babesia gibsoni* and evaluation of its diagnostic potential in an enzyme-linked immunosorbent assay. *J. Clin. Microbiol.* **39,** 2603–2609
37. Hines, S. A., Palmer, G. H., Jasmer, D. P., Goff, W. L., and McElwain, T. F. (1995) Immunization of cattle with recombinant *Babesia bovis* merozoite surface antigen-1. *Infect. Immun.* **63,** 349–352
38. Verdida, R. A., Hara, O. A., Xuan, X., Fukumoto, S., Igarashi, I., Zhang, S., Dong, J., Inokuma, H., Kabeya, H., Sato, Y., Moritomo, T., Maruyama, S., Claveria, F., and Nagasawa, H. (2004) Serodiagnosis of *Babesia gibsoni* infection in dogs by an improved enzyme-linked immunosorbent assay with recombinant truncated P50. *J. Vet. Med. Sci.* **66,** 1517–1521
39. Fukumoto, S., Xuan, X., Takabatake, N., Igarashi, I., Sugimoto, C., Fujisaki, K., Nagasawa, H., Mikami, T., and Suzuki, H. (2004) Inhibitory effect of antiserum to surface antigen P50 of *Babesia gibsoni* on growth of parasites in severe combined immunodeficiency mice given canine red blood cells. *Infect. Immun.* **72,** 1795–1798
40. Fukumoto, S., Tamaki, Y., Okamura, M., Bannai, H., Yokoyama, N., Suzuki, T., Igarashi, I., Suzuki, H., and Xuan, X. (2007) Prime-boost immunization with DNA followed by a recombinant vaccinia virus expressing P50 induced protective immunity against *Babesia gibsoni* infection in dogs. *Vaccine* **25,** 1334–1341